EurJOC
European Journal of Organic Chemistry

Research Article
doi.org/10.1002/ejoc.202201412

Chemistry Europe
European Chemical Societies Publishing

www.eurjoc.org

Special Collection

Reactivity Tuning of Metal-Free Artificial Photoenzymes through Binding Site Specific Bioconjugation

Thomas Kuckhoff,[a] Richard C. Brewster,[b] Calum T. J. Ferguson,*[a] and Amanda G. Jarvis*[b]

Amanda Jarvis was nominated to be part of this collection by EurJOC Board Member Andrew D. Smith

The design and development of artificial metal-free photoenzymes aims to combine the selectivity of enzymatic reactions with the benefits of modern synthetic photocatalysts. Removing the need for rare earth metals and allowing for milder reaction conditions, leading to a more sustainable catalytic system. Here, we present the design of a novel artificial photoenzyme by integrating an organophotocatalytic moiety based on a donor-acceptor design into a steroid carrier protein (SCP-2L). SCP-2L possesses a hydrophobic tunnel facilitating substrate binding in aqueous media. The photocatalyst was site-selectively bound to three SCP-2L variants, possessing a non-native cysteine residue strategically placed around the hydrophobic tunnel of the protein. The three modified photoenzymes were shown to be selective for the oxidation of organic sulfides giving up to 192 turnovers.

Introduction

Bioengineering allows the modification and functionalization of complex biomacromolecular structures and is a highly promising approach for developing efficient and sustainable catalysts using modified proteins and enzymes.[1] Enzymes are highly specific and efficient catalytic systems, combining stereoselectivity, biocompatibility, and stability, while having a limited substrate range. The three-dimensional nature of proteins allows for stereospecific hindrance near the active center, leading to highly selective catalytic processes, making protein scaffolds ideal platforms for the development of novel catalytic systems with the benefit of using water as a sustainable solvent. Through bioengineering, proteins can be combined with modern chemical catalysis leading to the synthesis of novel artificial enzymes and pairing the benefits of enzymatic precision, with the substrate range and capabilities of state-of-the-art chemical catalysts.[2]

Unfortunately, chemical synthesis and enzymatic conditions are often incompatible due to the need for high temperature, pressure, or organic solvents leading to the degradation of the biomaterial, making the optimization of conditions difficult.[3] Light is a renewable energy source and finds use in naturally occurring photoenzymes, removing the need for thermal energy.[4] Taking inspiration from nature, light-driven catalysis has undergone intensive research as an alternative and more sustainable way for chemical transformations.[5] Compared to traditional catalysts, photocatalysts utilize photosensitizing molecules, allowing light absorption and energy or electron transfer via the excited state, resulting in milder reaction conditions.

Due to their versatility, fully organic metal-free photocatalysts have found widespread application in photoredox reactions.[7] Recent developments aim to modify these photocatalysts to incorporate them into support materials to increase stability and combine the material properties of the supporting material with the photocatalyst. This has led to the development of various novel photocatalytic systems, including artificial photoenzymes.[8] The incorporation of a modified photocatalytic moiety into a protein combines the advantages of a protein structure with photocatalysis, developing a biocompatible, efficient, and sustainable catalytic system.[9] To control the active site placement and structure the catalyst is covalently bound to the protein, either through the usage of genetically encoded catalysts or site-selective bioconjugation.[8a,10] Recent examples from the groups of Green and Wu incorporated genetically encoded benzophenone into a Diels-Alderase and multidrug resistance regulator LmrR, demonstrating enantioselective [2 + 2] cycloadditions.[11] Lewis and coworkers modified a prolyl oligopeptidase protein POP with 9-mesityl-10-methylacridinium via click chemistry and showed the photoenzyme was active in sulfoxidation reactions.[12] Nevertheless, the efficient incorporation of photocatalytic moieties into proteins and the overall development of bioconjugated proteins with precisely engineered catalytic centers remains a significant challenge in designing artificial enzymes.

Due to its ability to sequester substrates, the human steroid carrier protein SCP-2L is an ideal scaffold for artificial enzymes. SCP-2L possesses a single domain made from 120 amino acids creating a hydrophobic tunnel, which allows for the uptake of

[a] T. Kuckhoff, Dr. C. T. J. Ferguson
Max Planck Institute for Polymer Research
Ackermannweg 10, 55128 Mainz (Germany)
E-mail: ferguson@mpip-mainz.mpg.de
[b] Dr. R. C. Brewster, Dr. A. G. Jarvis
School of Chemistry
University of Edinburgh
EH9 3FJ Edinburgh (United Kingdom)
E-mail: amanda.jarvis@ed.ac.uk

Supporting information for this article is available on the WWW under https://doi.org/10.1002/ejoc.202201412

Part of the "NextGenOrgChem" Special Collection.

Research Article
doi.org/10.1002/ejoc.202201412

apolar substrates.[13] The hydrophobic tunnel holds suitable positions for strategical positioning and introduction of non-native cysteine residues while previously solved crystal structures show that no structural changes occur due to the introduction of non-native cysteine residues compared to the wild-type protein.[14]

The incorporated photocatalytic moiety is based on a well-established donor-acceptor design allowing for better charge separation and an increased lifetime of the excited state. This photocatalytic design based on an electron-deficient benzothiadiazole unit allows control over HOMO/LUMO level depending on the chosen donor and acceptor units.[15] The 4,7-diphenyl-2,1,3-benzothiadiazole core has found widespread applications in conjugated frameworks,[16] homogeneous catalysis[15,17] or through incorporation into classical polymers,[18] catalyzing numerous light-driven photoreactions, including pollutant remediation,[19] photooxidation,[20] cycloaddition,[21] C–C coupling,[15] and bromination.[17]

Here, we report the design of novel artificial photoenzymes by integrating a photocatalytic 4,7-diphenyl-2,1,3-benzothiadiazole moiety into the protein SCP-2L, with the photocatalyst being bioconjugated at three unique cysteine residues within the protein (Scheme 1). The resulting photoenzymes were analyzed via LCMS, UV/Vis, and the photocatalytic activity of all three variants was investigated using selective oxidation of thioanisole.

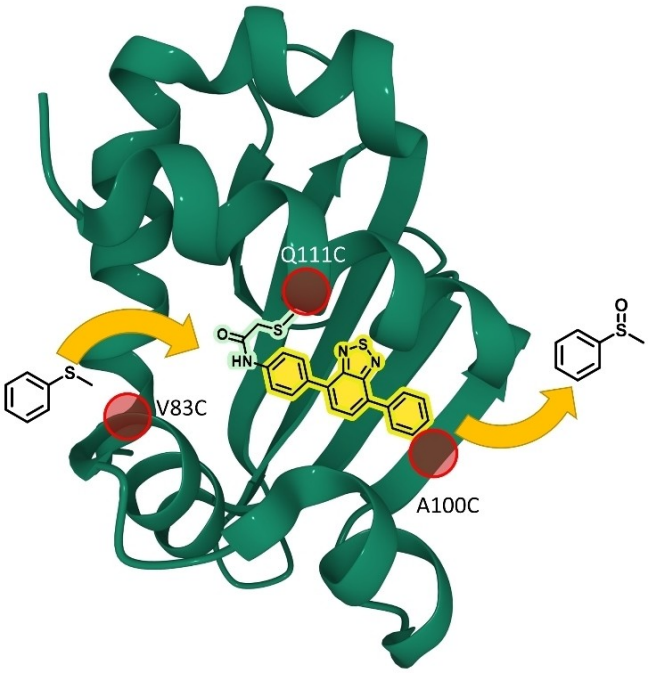

Scheme 1. Protein scaffold with highlighted positions of non-native cysteine variants A100C, V83C, and Q111C in combination with the bioconjugated photocatalytic moiety. Image created using Mol* and 1IKT from the RCSB PDB (rcsb.org).[6]

Results and Discussion

To incorporate the photocatalytic unit into the protein scaffold, non-native cysteine residues were first introduced into the wild-type protein by site directed mutagenesis, yielding three specific proteins SCP-2L A100C, SCP-2L Q111C, and SCP-2L V83C (hereafter referred to as A100C, Q111C and V83C).[13,22] V83C and A100C are positioned at either end of the hydrophobic tunnel, and Q111C was chosen due to its position in the center of the tunnel.[13b] (Scheme 1) In order to bioconjugate the 4,7-diphenyl-2,1,3-benzothiadiazole photocatalyst into the protein scaffold a reactive handle need to be introduced. To ensure a full bioconjugation, without any remaining non- or multiple conjugated proteins, three different functionalities for the photocatalyst with increasing reactivity were selected (Table 1). First, a vinyl-functionalized photocatalyst was synthesized with the goal of modifying the protein via a thiol-ene type coupling.[23] (Table 1, Entry 1) However, no reactivity was detected with either cysteine or V83 C using blue light or radical initiator VA-044.

Acrylamides are good Michael-acceptors and are commonly used in medicinal chemistry as non-covalent inhibitors as they react selectively with cysteine.[24] A photocatalyst with an acrylamide group was synthesized and reacted with all three SCP-2L variants (Table 1, Entry 2). After optimization of the bioconjugation reaction, stark differences in the incorporation yield depending on the positioning of the non-native cysteine residue were observed. V83C-2 was fully functionalized with the

Amanda Jarvis performed her undergraduate studies at the University of St Andrews (Scotland), before moving to the University of York to conduct her PhD studies. Following post-doctoral positions at the ICSN (Gif-sur-Yvette, France) and in St Andrews, she started her independent career in the School of Chemistry at the University of Edinburgh in 2017 supported by a Christina Miller fellowship. In 2019, she was subsequently awarded a UKRI Future Leaders Fellowship and in 2022 was promoted to Senior Lecturer. Her research focuses on the development of artificial enzymes as catalysts to help improve the overall sustainability of chemical synthesis.

Table 1. Synthesized photocatalyst and yield of incorporation.

	Photocatalyst	Photoenzyme	V83C	A100C	Q111C
1	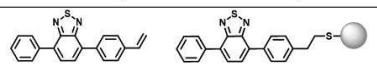		No conversion was observed[a]		
2	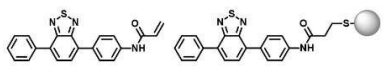		<98%[b]	<15%[b]	<49%[b]
3	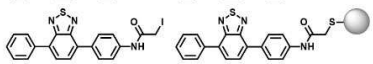		<99%[c]	<99%[c]	<99%[c]

[a] 100 μM protein 1 mM photocatalyst, blue light or VA-044, PBS (10% DMF), 37 °C, overnight [b] 50 μM protein,1 mM photocatalyst, HEPES buffer (50 mM HEPES, 50 mM NaCl, 10% DMF) pH 8.5, 20 °C overnight [c] 100 μM protein 1 mM photocatalyst, HEPES buffer (50 mM HEPES, 50 mM NaCl, 10% DMF) pH 8.5, 20 °C 1 h.

Research Article
doi.org/10.1002/ejoc.202201412

photocatalytic moiety showing no double or non-modified protein by LCMS (Figure S3).

However, A100C-2 and Q111C-2 could not be fully bioconjugated and showed remaining non-modified protein (Figure S3). These results demonstrate site-specific preferences assumingly due to the steric hindrance of the protein scaffold surrounding the cysteine residue. Interestingly the yield of modified Q111C-2 was higher than for A100 C-2, indicating an easy uptake of the hydrophobic photocatalyst into the apolar protein tunnel. Instead of opting for harsher conditions to increase the yield of the bioconjugation, the reactivity of the functional group was increased again. A photocatalyst with an iodoacetamide group was synthesized and used for bioconjugation (Table 1, Entry 3). A quick and efficient bioconjugation was observed using this modified photocatalyst, leading to a complete modification of all three positions within 60 min at room temperature. Due to the replaced amino acids, all three variants possess slight differences in their mass with A100C (13405 Da), Q111C (13349 Da), and V83C (13377 Da), respectively (Figure 1; Figure S2). The mass increases accordingly on the addition of the iodoacetamide functionalized photocatalyst by 343 Da, to give the following single modified photoenzymes A100C-3 (13748 Da), Q111C-3 (13691 Da), and V83C-3 (13720 Da). (Figure 1; Figure S4) The resulting bioconjugated proteins were analyzed via LCMS, showing no signs of non- or multiple modified proteins, and were consequentially used for analysis via UV/Vis and photocatalytic reactions.

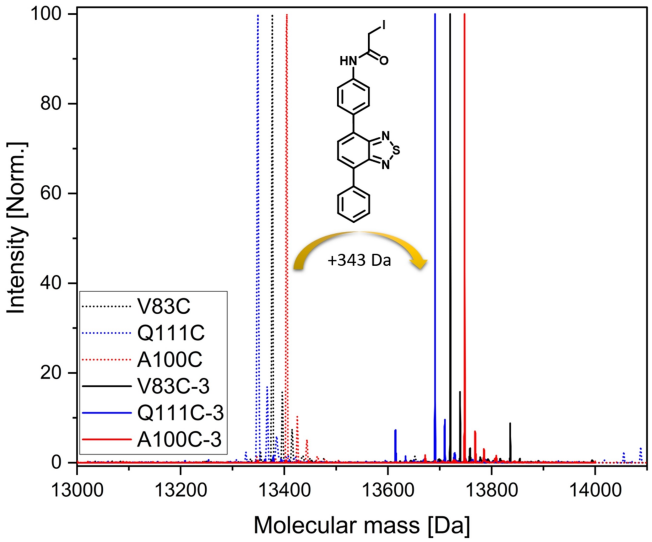

Figure 1. Mass spectra of all three variants A100C, V83C, and Q111C before and A100C-3, V83C-3 and Q111C-3 after bioconjugation via LC-MS.

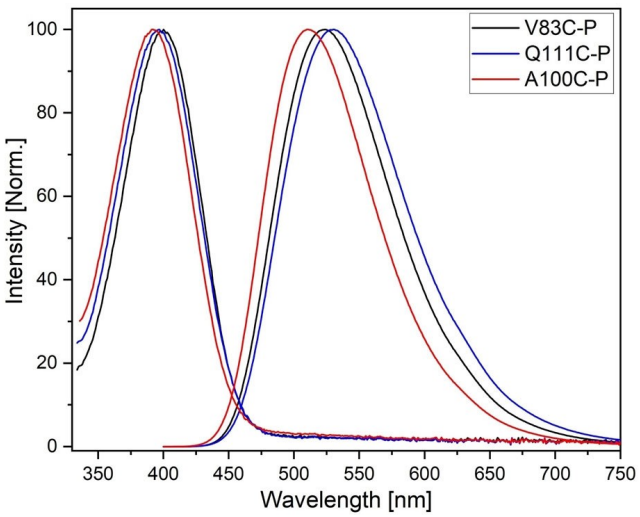

Entry	Protein	Absorbance	Emission	Stokes shift	Excitation
1	A100C-P	393	510	117	387
2	Q111C-P	397	530	133	390
3	V83C-P	400	524	124	398

Figure 2. Absorbance and emission spectra of A100C-3, Q111C-3, and A100C-3, as well as their corresponding peaks.

The resulting bioconjugated photoenzymes (A100C-3, V83C-3, Q111C-3) were first analyzed using UV/Vis-absorbance and fluorescence emission spectroscopy (Figure 2). Due to the different locations of the non-native cysteine residue and the bound photocatalytic moiety, slight shifts in the absorbance and emission are due to be expected. These shifts in the absorbance and emission can be explained due to the differences in the surrounding hydrophobic structure and neighboring amino acids creating slight differences in the protein environment. Compared to the non-conjugated protein, the bioconjugated photoenzymes showed strong visible light absorbance under 470 nm and a further peak in the UV range between 330–250 nm (Figures S5-6). A clear absorbance peak shift was observed depending on the position of bioconjugation. For example, A100C-3 had the lowest absorbance peak at 393 nm, followed by Q111C-3 at 397 nm. Over all three proteins, the absorbance shifted by 7 nm. Similar behavior could be observed for the emission spectra, with all variants displaying a broad emission spectrum between 420–750 nm. Interestingly the maximum emission varied largely with a shift range of 20 nm.

Q111C-3 possesses the highest emission peak and the most significant stokes-shift, while A100C-3 possesses the smallest stokes-shift paired with the lowest absorbance and emission peak. These observations highlight the influence of the position of the photocatalytic moiety at the entrance or center of the hydrophobic tunnel on the artificial enzyme photoproperties.

Further the photophysical properties of the synthesized photocatalytic moiety bound to a free cysteine was investigated through density fluctuation theory (DFT) calculations. (Figure S18) The HOMO/LUMO levels (−5.87/−2.67 eV) as well as the energy of the triplet state (1.79 eV) were calculated,and highlighted the possibility for the formation of singlet oxygen in the photoenzymes.[25] Consecutive performed electron paramagnetic resonance spectroscopy (EPR) using the bioconjugated V83C-3 and 2,2,6,6-tetramethylpiperidine as singlet oxygen trapping agent confirmed the singlet oxygen formation upon irradiation, showing photoresponsive behavior and indicating the possibility to promote photocatalytic reactions (Figure S19).

Research Article
doi.org/10.1002/ejoc.202201412

Chemistry Europe
European Chemical Societies Publishing

Sulfoxides are a common functional group in drug molecules, finding pharmaceutical application in proton-pump inhibitors or as an anti-inflammatories.[26] The selective photocatalytic oxidation of sulfides can be achieved in the presence of oxygen through formation of singlet oxygen.[27] Lewis and coworkers first reported the selective oxidation of thioanisole using an artificial photoenzymes achieving modest TON of under 20.[12] Comparable results were achieved by Brustad and coworkers, who synthesized a total of twelve artificial enzymes by incorporating functionalized 9-mesityl-10-phenyl acirindium photocatalysts into three modified protein scaffolds.[8c] Therefore, the catalytic activity of our artificial photoenzymes was investigated through photooxidation of a model sulfide in water (Table 2), and a kinetic study was conducted to analyze the effect of the binding site further (Figure 3; Figures S10–15). All three variants show high selectivity, and the organic sulfide was selectively oxidized to the sulfoxide showing no evidence for further oxidation to the sulfone, reaching conversions of up to 96%. Interestingly, it was found that the position of the photocatalytic moiety in the protein scaffold greatly affected the efficiency of the photoenzyme (Figure 3). The kinetic study shows a typical decrease in the conversion rate at higher yields, leading to near completion after eight hours, with significant differences in the reaction rate. The highest conversions were achieved by Q111C-3, which is positioned in the center of the hydrophobic tunnel, and V83C-3, with 95–96%. A significantly lower conversion can be observed with A100C-3, which like V83C-3, is positioned at the entrances of the hydrophobic tunnel (Scheme 1).

Although V83C-3 and Q111C-3 reach near full conversions after 8 h, different reaction rates can be observed for all three modifications within the first two hours, with V83C-3 having the highest initial rate. A100C-3 has, compared to its counterparts, the lowest initial rate combined with the lowest absorbance and emission peak and the smallest stoke shift setting it apart from V83C-3 and Q111C-3. Chiral sulfoxides are valuable pharmaceutical targets, and can show differences in the pharmacological activity depending on the stereo conformation. The oxidized sulfoxide formed possesses a chiral stereo center. Both stereoisomers were separated via chiral HPLC, but did nostereoselectivity was observed (Figure S16). This matches the previous observations by Lewis and Brustad who also did not observe a stereoselective oxidation, presumably due to the reaction mechanism depending on the formation of singlet oxygen.[8c,12]

Lastly, the stability of the created artificial photoenzymes were investigated. Six samples of V83C-3 were irradiated for up to 24 h prior to the photocatalytic reaction to analyze the photodeactivation and long-term stability of the photoenzyme. Upon long irradiation small amount of precipitation occurred which was removed though filtration before catalytic testing (Figure S20). The photoenzyme shows a high stability, with limited decreases in conversion only occurring after 8 h of irradiation. Even after 24 h of irradiation a conversion of 74% and a TON of 148 is still achieved (Figure S21).

Table 2. Efficiency comparison of bioconjugated photoenzyme A100C-3, Q111C-3 and V83C-3.

Number	SCP-2L	Conversion [%]	TON[a]
1	A100C-3	83	165
2	V83C-3	95	190
3	Q111C-3	96	192

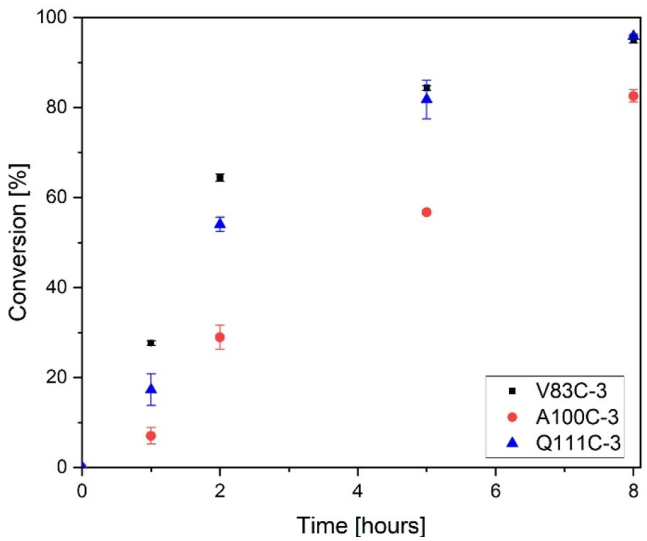

Figure 3. Photocatalytic oxidation of thioanisole; Conditions: Modified protein 10 μM, thioanisole 2 mM, MES buffer (MES 20 mM, 50 mM NaCl, 2% ACN) pH 6, blue light irradiation (460–465 nm) at room temperature; a) TON determination after eight hours. Conversion rate determined via GC-MS (measured in triplets Supporting Information.**11–15**).

Conclusion

In summary, we have produced a metal-free photoenzyme by incorporating a donor-acceptor based organophotocatalytic moiety into a modified SCP-2L protein scaffold. SCP-2L possesses a hydrophobic tunnel that we hypothesized could be an advantageous property in combination with a photocatalytic moiety, resulting in a water soluble photocatalyst. Three distinct variants of SCP-2L with non-native cysteine residue, A100C, V83C, and Q111C, were expressed and subsequently bioconjugated successfully with an iodoacetamide derivative of 4,7-diphenyl-2,1,3-benzothiadiazole to give the corresponding photoenzymes SCP-2L A100C-3, V83C-3 and Q111C-3. The effect of the position of bioconjugation on the optical properties of the photocatalyst was analyzed via UV/Vis, and the efficiency of the yielded photoenzymes was determined via photocatalytic oxidation of a model sulfide under visible light irradiation. The results showed significant differences in the reaction rate depending on the cysteine position, with A100C-3 having the lowest photocatalytic activity in combination with lower absorbance and emission peaks.

Research Article
doi.org/10.1002/ejoc.202201412

We believe this to be a promising start for the further development of photoenzymes based on incorporating photocatalytic moieties into SCP-2L based proteins. Combining the benefits of photocatalysis and biocatalysis, the synthesis of these novel catalytic systems eliminates the requirement for toxic materials, organic solvents, or non-degradable support material leading to sustainable photocatalytic reactions for the synthesis of high-value chemicals.

Experimental Section

General information; All chemicals were purchased from commercial sources and used without further purification. Analysis of proteins and modified proteins was performed via LC–MS(ES+) on a Waters Acquity I–Class UPLC coupled to a Waters Synapt G2 HDMS and the results were analysed via MassLynx V. 4.0. Yield for incorporation of *N*-(4-(7-phenyl benzo[c][1,2,5]thiadiazol-4-yl)phenyl)acrylamide was calculated by mass peak count ratio (± 1 Da). UV/Vis absorbance spectroscopy was measured on a Cary 50 UV − Vis/NIR spectrometer and fluorescence emission on a RF-6000 – Shimadzu using LabSolutions RF. ^{1}H and ^{13}C NMR spectra were measured using a Bruker Pro 500 operating at 500 MHz or 126 MHz respectively and analysed via MestReNova. Gas chromatography was performed on a Shimadzu GC-2010 plus gas chromatograph and analysed with a QP2010 ultra mass spectrometer, using a ZB-5MS column with helium as carrier gas. Integration of starting material and product peak is used to determine the conversion ratio while using anisole as reference. Chiral HPLC was measured on an Agilent Series 1200 using a Daicel Chiralpak IE 250 mm/4.6 mm/5 μm column in THF/n-hexane 20/80. Mass spectroscopy was measured on an Advion Expression LCMS using (APCI) and was analysed using Advion data express. DFT calculations were performed using Gaussian 16. The DFTs for the HOMO/LUMO levels were calculated for optimisation of local minimum using method rb3lyp/6-31 + g(d) the triplet state energy was calculated for optimisation of local minimum using method b3lyp/6-31 + g(d). Frontier molecular orbitals pictures were produced using Avogadro. Electron Paramagnetic Resonance spectroscopy was performed on a Magnettech Miniscope MS200 spectrometer at room temperature, microwave frequency: 9.391 GHz, scan time: 60 s. Photocatalytic reactions were performed using 24 V super bright LED tape, blue 460–465 nm, 18 W, from Ultra LEDS. All graphs and figures were created using OriginPro 2019b, chemical structures were drawn in ChemDraw 20.1.

Protein purification and expression: The mutagenesis, expression and purification of the protein variants was carried out as previously reported.[13,22]

General method for bioconjugation: All protein variants were modified after the same procedure. Purified protein was defrosted and taken up in HEPES buffer (50 mM HEPES, 50 mM NaCl, 8.5 pH) to a concentration of 100 μM. 10 equivalents of 2-iodo-N-(4-(7-phenylbenzo[c][1,2,5]thiadiazol-4-yl)phenyl)acetamide (stock solution: 10 mM in DMF) were added. The solution was incubated in a thermoshaker (20 °C, 1 h, 300 rpm). The Eppendorf was then centrifuged (12k, rt, 5 min) twice, each time the precipitate was discarded. The supernatant was filtered, centrifuged again and then purified over a PD-10 desalting column (MES buffer 20 mM, 50 mM NaCl, 6 pH). If the solution volume exceeded the recommended volume of the desalting column a centrifugation filter (10 kDa cut-off, Amicon) was used to concentrate the solution and diluted again afterwards. The final concentration was determined via a Bradford assay.[28]

Photocatalytic oxidation: Modified SCP-2L protein (10 nmol) in MES buffer (20 mM MES, 50 mM NaCl, 1 mL) at pH 6 is added to a glass vial. The organic sulfide was dissolved in acetonitrile (100 mM) and 20 μL (2 μmol) are added to the vial. The vial was capped and placed in the photoreactor. The samples were irradiated with blue LED light (460-465 nm, 18 W) for a set time period. After irradiation, the solution was extracted three times with DCM, dried over $MgSO_4$ and analysed via GC/MS.

Photostability test: Modified SCP-2L protein (20 nmol) in MES buffer (20 mM MES, 50 mM NaCl, 2 mL) at pH 6 is added to a glass vial and irradiated with blue light for up to 24 h under room temperature. The samples are filtered and 1 mL (SCP-2L 10 nmol) is used for photocatalytic testing. The organic sulfide was dissolved in acetonitrile (100 mM) and 20 μL (2 μmol) are added to the vial. The vial was capped and placed in the photoreactor. The samples were irradiated for 8 h under blue light, extracted three times with DCM dried over $MgSO_4$ and analysed via GC/MS.

Synthesis: 4-phenyl-7-(4-vinylphenyl)benzo[c][1,2,5]thiadiazole (Table 1 Entry 1) and *N*-(4-(7-phenyl benzo[c][1,2,5]thiadiazol-4-yl)phenyl)acryl amide (Table 1 Entry 2) were performed and purified after previously published procedures.[20,21]

Synthesis of 2-iodo-*N*-(4-(7-phenylbenzo[c][1,2,5]thiadiazol-4-yl) phenyl)acetamide: Phenylboronic acid (553 mg, 4.54 mmol, 1.00 equiv.), 4,7-dibromobenzo[c][1,2,5]thiadiazole (2 g, 6.80 mmol, 1.50 equiv.), $Pd(PPh_3)_4$ (157 mg, 136 μmol, 0.03 equiv.), Na_2CO_3 (1.7 g, 15.96 mmol) were added to a Schlenk tube and evacuated. Toluene (18 mL), ethanol (8 mL) and water (8 mL) were degassed via nitrogen bubbling for 20 min. The Schlenk tube was filled with nitrogen, the solvents were added and the solution was vigorously stirred (90 °C, 24 h). After reaching room temperature, the solution was extracted with dichloromethane and the combined organic phases were washed with brine, dried over anhydrous $MgSO_4$, concentrated and the catalyst was removed over silica column chromatography (PE/DCM gradient 4 : 1→0 : 1).

Step 2: The crude product from step 1 (330 mg), 4-(4,4,5,5-tetramethyl-1, 3,2-dioxaborolan-2-yl)aniline (270 mg, 1.29 mmol, 1.10 equiv.), $Pd(PPh_3)_4$ (99 mg, 85.9 μmol, 0.05 equiv.), Na_2CO_3 (0.63 g, 5.95 mmol) were transferred into a Schlenk tube and evacuated. 1,4-Dioxane (7.5 mL) and H_2O (3 mL) were degassed using nitrogen over 20 min. The Schlenk tube was backfilled with nitrogen and the solvents were added. The solution was stirred at 100 °C overnight. The resulting mixture was extracted with dichloromethane and the combined organic phases were washed with brine (50 mL), dried over anhydrous $MgSO_4$ and concentrated using a rotary evaporator. The crude product was then purified by column chromatography on silica gel (PE/DCM gradient 2:1→0:1). The column was further pretreated with DCM / 5 vol.% TEA). The product was yielded as red crystals (191 mg, 0.63 mmol, 56% yield), in linewith previously reported results.[20]

H NMR (300 MHz, CD_2Cl_2): δ = 8.02–7.92 (m, 2H), 7.84 (d, 2H), 7.75 (q, 2H), 7.53 (t, 2H), 7.44 (t, 1H), 6.84 (d, 2H), 3.95 ppm (s, 2H).

Step 3: To a dried Schlenk tube 4-(7-phenyl-benzo[c][1,2,5]thiadiazol-4-yl)aniline (100 mg, 330 μmol, 1.00 equiv.), triethylamine (69 μL, 494 μmol, 1.5 equiv.) and dry THF (2 mL) were added. The solution was stirred at room temperature for 10 min before being cooled to 0 °C. A stock solution of chloroacetyl chloride (39.5 μL, 494 μmol, 1.50 equiv.) in dry THF (2 mL) was prepared and slowly added overtime. The solution slowly changed color from red to yellow/brown. The solution was stirred at room temperature overnight and was then quenched with water and extracted with DCM. The combined organic fractions were washed with water and dried over $MgSO_4$. The

solvent was evaporated and the product was washed with n-hexane and used without further purification.

Step 4: The starting materials 2-chloro-N-(4-(7-phenylbenzo[c][1,2,5]thiadiazol-4-yl)phenyl)acetamide (113 mg, 297 μmol) and KI (74 mg, 446 μmol) were transferred into a flame dried flask and dispersed in dry benzene. The solution was then freeze-dried. Around 80 mL of dry acetone were added and the flask was refluxed overnight. The solvent was evaporated and the solid taken up in DCM and washed with water. The water phase was extracted with DCM and the organic phases were combined. The solvent was evaporated and the product was washed with n-hexane, yielding the product as orange powder (65 mg, 138 μmol = 41 % yield over two steps)

^{1}H NMR (500 MHz, DMSO): $\delta = 10.52$ (s, 1H), 8.07–7.98 (m, 4H), 7.94 (s, 2H), 7.80–7.71 (m, 2H), 7.60–7.52 (m, 2H), 7.51–7.44 (m, 1H), 3.89 ppm (s, 2H).

^{13}C NMR (126 MHz, DMSO): $\delta = 167$, 153, 153, 139, 137, 132, 132, 130, 129, 129, 128, 128, 128, 119, 2 ppm.

MS *m/z*: 268.9, 301.0, 304.0, 345.0, 346.1, 347.0 471.9 $[M+H]^+$, 473.7, 475.7

Supporting Information includes ^{1}H/^{13}C NMR, mass-spectra, LCMS/GCMS Data, UV/Vis-spectra.

Acknowledgements

T.K. acknowledge ScotCHEM and the funding received from the Scottish Government under the SFC Saltire Emerging Researcher ScotCHEM European Exchanges Scheme. A.G.J. and R.C.B. were funded through a UKRI Future Leaders Fellowship (grant no. MR/S017402/1) awarded to A.G.J. A.G.J also acknowledges support from the Royal Society through RGS\R2\212138. We acknowledge access to mass spectrometry facilities through SIRCAMS at University of Edinburgh. R.C.B is currently an employee of AstraZeneca.

Conflict of Interest

The authors declare no conflict of interest.

Data Availability Statement

The data that support the findings of this study are available in the supplementary material of this article.

Keywords: Benzothiadiazole · Bioconjugation · Photocatalysis · Photoenzymes · Sulfoxidation

[1] a) R. C. Brewster, E. Klemencic, A. G. Jarvis, *J. Inorg. Biochem.* **2021**, *215*, 111317; b) K. Chen, F. H. Arnold, *Nat. Catal.* **2020**, *3*, 203–213; c) F. Schwizer, Y. Okamoto, T. Heinisch, Y. Gu, M. M. Pellizzoni, V. Lebrun, R. Reuter, V. Kohler, J. C. Lewis, T. R. Ward, *Chem. Rev.* **2018**, *118*, 142–231; d) A. G. Jarvis, *Curr. Opin. Chem. Biol.* **2020**, *58*, 63–71.

[2] a) H. J. Davis, T. R. Ward, *ACS Cent. Sci.* **2019**, *5*, 1120–1136; b) T. Matsuo, S. Hirota, *Bioorg. Med. Chem.* **2014**, *22*, 5638–5656.

[3] a) K. M. Polizzi, A. S. Bommarius, J. M. Broering, J. F. Chaparro-Riggers, *Curr. Opin. Chem. Biol.* **2007**, *11*, 220–225; b) M. M. Kristjánsson, J. E. Kinsella, in *Advances in Food and Nutrition Research, Vol. 35* (Ed.: J. E. Kinsella), Academic Press, **1991**, pp. 237–316; c) P. D. Patil, S. S. Nadar, D. T. Marghade in *Advances in Green Synthesis: Avenues and Sustainability* (Eds.: Inamuddin, R. Boddula, M. I. Ahamed, A. Khan), Springer International Publishing, Cham, **2021**, pp. 173–189.

[4] a) K. Brettel, M. Byrdin, *Curr. Opin. Struct. Biol.* **2010**, *20*, 693–701; b) M. Gabruk, B. Mysliwa-Kurdziel, *Biochem.* **2015**, *54*, 5255–5262; c) D. Sorigué, B. Légeret, S. Cuiné, S. Blangy, S. Moulin, E. Billon, P. Richaud, S. Brugière, Y. Couté, D. Nurizzo, P. Müller, K. Brettel, D. Pignol, P. Arnoux, Y. Li-Beisson, G. Peltier, F. Beisson, *Science* **2017**, *357*, 903–907.

[5] a) M. J. Genzink, J. B. Kidd, W. B. Swords, T. P. Yoon, *Chem. Rev.* **2022**, *122*, 1654–1716; b) M. H. Shaw, J. Twilton, D. W. MacMillan, *J. Org. Chem.* **2016**, *81*, 6898–6926; c) P. Li, J. A. Terrett, J. R. Zbieg, *ACS Med. Chem. Lett.* **2020**, *11*, 2120–2130.

[6] a) A. M. Haapalainen, D. M. van Aalten, G. Merilainen, J. E. Jalonen, P. Pirila, R. K. Wierenga, J. K. Hiltunen, T. Glumoff, *J. Mol. Biol.* **2001**, *313*, 1127–1138; b) D. Sehnal, S. Bittrich, M. Despande, R. Svobodová, K. Berka, V. Bazgier, S. Velankar, S. K. Burley, J. Koča, A. S. Rose, *Nucleic Acids Res.* **2021**, *49*, W431-W437.

[7] a) S. Fukuzumi, K. Ohkubo, *Chem. Sci.* **2013**, *4*, 561–574; b) N. A. Romero, D. A. Nicewicz, *Chem. Rev.* **2016**, *116*, 10075–10166; c) V. Srivastava, P. P. Singh, *RSC Adv.* **2017**, *7*, 31377–31392.

[8] a) X. Liu, F. Kang, C. Hu, L. Wang, Z. Xu, D. Zheng, W. Gong, Y. Lu, Y. Ma, J. Wang, *Nat. Chem.* **2018**, *10*, 1201–1206; b) N. H. Tran, D. Nguyen, S. Dwaraknath, S. Mahadevan, G. Chavez, A. Nguyen, T. Dao, S. Mullen, T. A. Nguyen, L. E. Cheruzel, *J. Am. Chem. Soc.* **2013**, *135*, 14484–14487; c) T. D. Schwochert, C. L. Cruz, J. W. Watters, E. W. Reynolds, D. A. Nicewicz, E. M. Brustad, *ChemBioChem* **2020**, *21*, 3146–3150.

[9] a) P. T. Cesana, B. X. Li, S. G. Shepard, S. I. Ting, S. M. Hart, C. M. Olson, J. I. Martinez Alvarado, M. Son, T. J. Steiman, F. N. Castellano, A. G. Doyle, D. W. C. MacMillan, G. S. Schlau-Cohen, *Chem* **2022**, *8*, 174–185; b) Y. Fu, J. Huang, Y. Wu, X. Liu, F. Zhong, J. Wang, *J. Am. Chem. Soc.* **2021**, *143*, 617–622; c) S. H. Mejias, G. Roelfes, W. R. Browne, *Phys. Chem. Chem. Phys.* **2020**, *22*, 12228–12238.

[10] Y. S. Zubi, B. Liu, Y. Gu, D. Sahoo, J. C. Lewis, *Chem. Sci.* **2022**, *13*, 1459–1468.

[11] a) J. S. Trimble, R. Crawshaw, F. J. Hardy, C. W. Levy, M. J. B. Brown, D. E. Fuerst, D. J. Heyes, R. Obexer, A. P. Green, *Nature* **2022**, *611*, 709–714; b) N. Sun, J. Huang, J. Qian, T. P. Zhou, J. Guo, L. Tang, W. Zhang, Y. Deng, W. Zhao, G. Wu, R. Z. Liao, X. Chen, F. Zhong, Y. Wu, *Nature* **2022**, *611*, 715–720.

[12] Y. Gu, K. Ellis-Guardiola, P. Srivastava, J. C. Lewis, *ChemBioChem* **2015**, *16*, 1880–1883.

[13] a) A. G. Jarvis, L. Obrecht, P. J. Deuss, W. Laan, E. K. Gibson, P. P. Wells, P. C. J. Kamer, *Angew. Chem. Int. Ed.* **2017**, *56*, 13596–13600; *Angew. Chem.* **2017**, *129*, 13784–13788; b) H. T. Imam, A. G. Jarvis, V. Celorrio, I. Baig, C. C. R. Allen, A. C. Marr, P. C. J. Kamer, *Catal. Sci. Technol.* **2019**, *9*, 6428–6437.

[14] M. V. Doble, L. Obrecht, H.-J. Joosten, M. Lee, H. J. Rozeboom, E. Branigan, J. H. Naismith, D. B. Janssen, A. G. Jarvis, P. C. J. Kamer, *ACS Catal.* **2021**, *11*, 3620–3627.

[15] L. Wang, W. Huang, R. Li, D. Gehrig, P. W. Blom, K. Landfester, K. A. Zhang, *Angew. Chem. Int. Ed.* **2016**, *55*, 9783–9787; *Angew. Chem.* **2016**, *128*, 9935–9940.

[16] a) R. Li, J. Byun, W. Huang, C. Ayed, L. Wang, K. A. I. Zhang, *ACS Catal.* **2018**, *8*, 4735–4750; b) R. Li, B. C. Ma, W. Huang, L. Wang, D. Wang, H. Lu, K. Landfester, K. A. I. Zhang, *ACS Catal.* **2017**, *7*, 3097–3101; c) C. Ayed, L. Caire da Silva, D. Wang, K. A. I. Zhang, *J. Mater. Chem. A* **2018**, *6*, 22145–22151.

[17] R. Li, D. W. Gehrig, C. Ramanan, P. W. M. Blom, F. F. Kohl, M. Wagner, K. Landfester, K. A. I. Zhang, *Adv. Synth. Catal.* **2019**, *361*, 3852–3859.

[18] a) C. T. J. Ferguson, K. A. I. Zhang, *ACS Catal.* **2021**, *11*, 9547–9560; b) C. T. J. Ferguson, N. Huber, T. Kuckhoff, K. A. I. Zhang, K. Landfester, *J. Mater. Chem. A* **2020**, *8*, 1072–1076.

[19] T. Kuckhoff, K. Landfester, K. A. I. Zhang, C. T. J. Ferguson, *Chem. Mater.* **2021**, *33*, 9131–9138.

[20] C. T. J. Ferguson, N. Huber, K. Landfester, K. A. I. Zhang, *Angew. Chem. Int. Ed.* **2019**, *58*, 10567–10571; *Angew. Chem.* **2019**, *131*, 10677–10681.

[21] N. Huber, R. Li, C. T. J. Ferguson, D. W. Gehrig, C. Ramanan, P. W. M. Blom, K. Landfester, K. A. I. Zhang, *Catal. Sci. Technol.* **2020**, *10*, 2092–2099.

[22] P. J. Deuss, G. Popa, C. H. Botting, W. Laan, P. C. Kamer, *Angew. Chem. Int. Ed.* **2010**, *49*, 5315–5317; *Angew. Chem.* **2010**, *122*, 5443–5445.

[23] A. K. Sinha, D. Equbal, *Asian J. Org. Chem.* **2019**, *8*, 32–47.
[24] J. S. Martin, C. J. MacKenzie, D. Fletcher, I. H. Gilbert, *Bioorg. Med. Chem.* **2019**, *27*, 2066–2074.
[25] C. Schweitzer, R. Schmidt, *Chem. Rev.* **2003**, *103*, 1685–1758.
[26] a) R. Bentley, *Chem. Soc. Rev.* **2005**, *34*, 609–624; b) A. S. Surur, L. Schulig, A. Link, *Arch. Pharm.* **2019**, *352*, e1800248; c) F. Xiong, B. B. Yang, J. Zhang, L. Li, *Molecules* **2018**, *23*, 2680.
[27] E. Skolia, P. L. Gkizis, C. G. Kokotos, *ChemPlusChem* **2022**, *87*, e202200008.
[28] M. M. Bradford, *Anal. Biochem.* **1976**, *72*, 248–254.

Manuscript received: November 30, 2022
Revised manuscript received: February 7, 2023
Accepted manuscript online: February 13, 2023